HHS Public Access

Author manuscript

Invest Radiol. Author manuscript; available in PMC 2019 October 01.

Published in final edited form as:

Invest Radiol. 2018 October ; 53(10): 587–595. doi:10.1097/RLI.0000000000000465.

Diffusion-weighted Imaging with Apparent Diffusion Coefficient Mapping for Breast Cancer Detection as a Stand-Alone-Parameter: Comparison with Dynamic Contrast-enhanced and Multiparametric Magnetic Resonance Imaging

Katja Pinker[1,2], **Linda Moy**[3], **Elizabeth J Sutton**[1], **Ritse M Mann**[4], **Michael Weber**[2], **Sunitha B Thakur**[1], **Maxine S Jochelson**[1], **Zsuzsanna Bago-Horvath**[5], **Elizabeth A Morris**[1], **Pascal AT Baltzer**[1], and **Thomas H Helbich**[2]

[1]Department of Radiology, Breast Imaging Service, Memorial Sloan Kettering Cancer Center, NY, New York, USA [2]Department of Biomedical Imaging and Image-guided Therapy, Division of Molecular and Gender Imaging, Medical University of Vienna, Vienna, Austria [3]Center for Advanced Imaging Innovation and Research, Laura and Isaac Perlmutter Cancer Center, New York University of Medicine, New York, USA [4]Department of Radiology, Radboud University Nijmegen, Nijmegen, the Netherlands [5]Department of Pathology, Medical University of Vienna, Vienna, Austria

Abstract

Purpose—To compare dynamic contrast-enhanced magnetic resonance imaging (DCE-MRI) to diffusion weighted imaging (DWI) with apparent diffusion coefficient (ADC) mapping as a stand-alone parameter without any other supportive sequence for breast cancer detection and to assess its combination as multiparametric (mp)MRI of the breast.

Materials and Methods—In this institutional review board approved single-center study prospectively acquired data of 106 patients who underwent breast MRI from 12/2010–09/2014 for an imaging abnormality (BI-RADS 0, 4/5) were retrospectively analysed. Four readers independently assessed DWI and DCE as well as combined as mpMRI. BI-RADS categories, lesion size and mean ADC values were recorded. Histopathology was used as the gold standard. Appropriate statistical tests were used to compare diagnostic values.

Results—There were 69 malignant and 41 benign tumors in 106 patients. Four patients presented with bilateral lesions. DCE-MRI was the most sensitive test for breast cancer detection with an average sensitivity of 100%. DWI alone was less sensitive (82%($p<0.001$)) but more specific than DCE-MRI (86.8% vs. 76.6%($p=0.002$)). Diagnostic accuracy was 83.7% for DWI and 90.6% for DCE-MRI. mpMRI achieved a sensitivity of 96.8%, not statistically different from DCE-MRI ($p=0.12$) and with a similar specificity as DWI (83.8%($p=0.195$)) maximizing diagnostic accuracy to 91.9%. There was almost perfect inter-reader agreement for DWI ($\kappa=0.864$) and DCE-MRI ($\kappa=0.875$) for differentiation of benign and malignant lesions.

Corresponding author: Katja Pinker, MD, PhD, Department of Radiology, Breast Imaging Service, Memorial Sloan Kettering Cancer Center, 1275 York Avenue, New York, NY 10065, USA, Phone: 646 888 5489, pinkerdk@mskcc.org.

Conclusion—DCE-MRI is most sensitive for breast cancer detection and thus still indispensable. mpMRI using DCE-MRI and DWI maintains a high sensitivity, increases specificity and maximizes diagnostic accuracy, often preventing unnecessary breast biopsies. DWI should not be used as a stand-alone parameter because it detects significantly fewer cancers in comparison to DCE-MRI and mpMRI.

Introduction

Dynamic contrast-enhanced magnetic resonance imaging (DCE-MRI) is the back-bone of any breast MRI imaging protocol and the most sensitive imaging test for breast cancer detection (1, 2). With the recent controversy and the concerns about the safety of about gadolinium containing contrast agents (3), the recommendations that “gadolinium based contrast agents should only be administered if the information so provided is necessary, and specifically expected to increase the confidence in correct disease diagnosis or assessment thereof, or disease exclusion”(4). Several unenhanced MR imaging parameters spanning the spectrum from diffusion-weighted imaging to sodium imaging (5-7) have been explored to detect breast cancer, with encouraging results. Of all these MRI parameters, diffusion-weighted imaging (DWI) has emerged as the most robust and reliable for routine clinical use. With significant advances in hardware and sequence technology such as the use of higher field strengths and readout-segmented DWI sequences, sensitivities of DWI using apparent diffusion coefficient (ADC) mapping of up to 96% for breast cancer detection and specificities of up to 100% for breast tumor characterization have been reported (6, 8-11). It has therefore been suggested that unenhanced imaging with DWI might replace DCE-MRI in for breast cancer detection (12-16). However, it must be stressed that most of the studies used a combination of either DCE-MRI, unenhanced T1-weighted and/or T2-weighted imaging with DWI(12, 14-21). In this setting DWI was not used as a single stand-alone parameter and the potentials of unenhanced DWI may therefore be overestimated. In contrast, several authors have investigated the combined use of DWI and DCE-MRI, which is defined as multiparametric (mp)MRI, for improved breast lesion detection and characterization with excellent results (22-25). Therefore, the primary goal of this study was to clarify whether DWI without any other supportive sequence achieves a sensitivity equal to DCE-MRI for breast cancer detection and thus can be used as a stand-alone parameter. As a secondary goal, we aimed to prove that as both DCE-MRI and DWI have their individual limitations, the best approach for reliable breast cancer diagnosis while avoiding unnecessary breast biopsies is their combination as mpMRI.

Materials and Methods

In this institutional review board-approved single-institution study at __, prospectively acquired data, where all patients gave written, informed consent, were retrospectively analysed.

Patients

A prospectively populated research database was searched for patients who underwent state-of–the-art multiparametric MRI of the breast with T2-weighted, DCE-MRI and DWI from 12/2010–09/2014 and fulfilled the following inclusion criteria: ≥18 years; not pregnant; not

breastfeeding; suspicious finding at mammography or breast ultrasonography, i.e., asymmetric density, architectural distortion, breast mass, or microcalcifications [(Breast Imaging Reporting and Data System [(BI-RADS) 0, further imaging warranted; 4, suspicious abnormality; 5, highly suggestive for malignancy)]; no previous treatment; and no contraindications for MRI or MRI contrast agents. Patients were excluded if there was no histopathologic verification of the imaging findings by either image-guided or surgical biopsy or if severe movement or susceptibility artifacts were seen on either DWI or DCE-MR images. Based on a sample size calculation (refer to Statistical Analysis section) 106 out of 1119 patients were randomly selected using the selection criteria of lesion size ≧5mm on DCE-MRI and a distribution of at least one-third benign breast tumors. In all patients, electronic medical records were reviewed and the following patient characteristics were recorded: age; pathology and in malignant lesions tumor grade; receptor status; and molecular subtype based on immunohistochemical surrogates. Nineteen patients examined in this study have been previously analyzed in a different context (26).

Imaging

All patients underwent breast MRI in the prone position using a 3T scanner (Tim Trio, Siemens, Erlangen, Germany) and a four-channel breast coil (InVivo, Orlando, FL, USA). A standardized MRI protocol was performed with the following sequences:

A T2-weighted turbo spin echo sequence with fat suppression: time of repetition (TR)/time of echo (TE) 4800/59 msec; field of view (FOV) 340mm; 44 slices at 4mm; flip angle 120°; matrix 384×512; and acquisition time (TA) 2:35min.

For DWI axial three-acquisition trace diffusion-weighted, double-refocused, single-shot echo-planar imaging (EPI) with inversion recovery fat suppression (TR/TE/time of inversion (TI) 8000/59/210 ms; FOV 360×202mm; 24 slices at 5mm; intersection gap (%) 10, matrix 172×96 [50% oversampling]; b-values 50 and 850s/mm, TA 2:56min) was performed (9).

For DCE-MRI until 12/2011 a hybrid DCE-MRI protocol was used (27). The protocol consisted of five alternating sections of high-spatial and high-temporal resolution T1-weighted sequences. First, a high spatial resolution, pre-contrast coronal T1-weighted turbo fast-low-angle-shot-(FLASH)-3D sequences without preparation pulse and with selective water-excitation (TR/TE 877/3.82 ms; FOV 320 mm; 96 slices; 1 mm isotropic; matrix 320×134; one average; bandwidth 200 Hz/pixel; 2 min) was acquired. Subsequently a coronal T1-weighted Volume-Interpolated-Breathhold-Examination (VIBE) sequences (TR/TE 3.61/1.4 ms; FOV 320 mm; 72 slices; 1.7 mm isotropic; matrix 192×192; one average; bandwidth 400 Hz/pixel; 13.2 s per volume) for the optimal assessment of the contrast-enhancement kinetics of lesions, was obtained. We performed 17 measurements including baseline scan as the peak enhancement of the lesion could be expected at the end of this time-span. Thereafter, contrast-enhanced, high spatial resolution T1-weighted images (repeated 3D-FLASH) for optimal image quality at expected maximum contrast were acquired. Finally, the high temporal resolution (repeated VIBE with 25 measurements, leading to an acquisition time of 5 min 35 secs and repeated 3D-FLASH) for dynamic assessment of lesion wash-out, and then, high spatial resolutionT1-weighted images and

delayed contrast-enhanced lesion morphology were recorded. The total time of acquisition was 9:20min.

From 01/2012 onwards a transversal T1-weighted time-resolved angiography with stochastic trajectories (TWIST) was acquired [water excitation fat-saturation; TR/TE 6.23ms/2.95ms; flip angle 15°, FOV 196 × 330mm2; 144 slices; spatial resolution 0.9 × 0.9 × 1mm; temporal interpolation factor 2; temporal resolution 14s; matrix 384 × 384; one average; center k-space region with a resampling rate of 23%; reacquisition density of peripheral k-space 20%; and TA 6:49min.

A standard dose (0.1mmol/kg body-weight) of Gadotaremeglumine (Gd-DOTA; Dotarem®, Guerbet, France) was injected intravenously as a bolus at 4ml/s with a saline flush after injection. Total MRI examination time was approximately 12-16 minutes.

Image analysis

Four breast radiologists (__ [r1], 12 years, __ [r2], 16 years, __ [r3], 5 years, __ [r4], 11 years of experience in breast MRI) independently evaluated DWI, DCE and mpMRI. T2-weighted imaging was not used for analysis and b 0 images of DWI were used to provide t2-weighted imaging contrast. Lesion location by clock position and depth per BI-RADS was recorded Readers first assessed DWI alone blinded to the DCE-MRI. After wash-out time period of at least 21 days DCE-MRI alone was read. Consequently, results of both readings were reviewed by r1 for missed lesion on DWI or a lesion mis-match between DCE-MRI and DWI. In case of mis-matched lesions or lesions missed in DWI the ADC values for these were measured. Finally, mpMRI results were derived using the algorithm described below. All readers were aware that all patients had a breast lesion, but were not provided with conventional and prior imaging or histopathological results.

DWI—High b-value (i.e., 850s/mm^2) images were qualitatively assessed for hyperintense regions. One two-dimensional region of interest per lesion and per reader was drawn manually on ADC maps on the area with the lowest ADC values inside the lesions (28), using OSIRIX® software (29) and the mean ADC of lesions was determined. A previously published ADC cut-off value of 1.25×10^{-3}mm^2/s (30) was used to differentiate between benign and malignant lesions.

DCE-MRI—DCE-MRI were evaluated using the 5th edition MRI BI-RADS lexicon (31). Size, location, type of enhancement [(mass or non-mass enhancement (NME)], morphologic descriptors for masses and NME and kinetics according to BI-RADS were recorded. For the kinetic curve assessment, an automated semi-quantitative curve-type analysis was performed using the DCE Tool plugin v2.2 for OSIRIX® (29). Average lesion sizes are reported for r1. Examinations were classified as either definitively benign (no indication of malignancy) or abnormal (suspicious finding, histopathologic verification necessary) and a BI-RADS assessment category (1-5) was assigned.

mpMRI—mpMRI with DWI and DCE-MRI was evaluated using a previously published reading method where BI-RADS values are adapted using different ADC thresholds for different BI-RADS categories to account for the higher likelihood of malignancy in lesions

with a higher BI-RADS assessment category (25). ADC thresholds for masses and NME for different BI-RADS categories are summarized in Table 1. A final classification as either definitively benign or abnormal was given. If a BI-RADS 4 or 5 was assigned on DCE-MRI, a high ADC (>1.39 or >1.66 for masses and >1.28 or >1.62 for NME) (Table 1) was required to assign a final classification as benign. If a BI-RADS 2 or 3 was assigned, a low ADC (<0.87 or <1.13 for masses and <0.62 or <0.95 for NME) (Table 1) was required to assign a final classification as malignant.

Standard of Reference

Preferentially histopathology was used as the reference standard. Histopathologic diagnosis was established by one experienced pathologist (__) using either image-guided needle biopsy or surgery. In case of a high-risk lesion (regarded as benign), the final diagnosis was established with surgery (n=7). In lesions suspicious in DWI yet without any enhancement (n=4: r1 n=2, r2 n=2, r3 n=1, r4 n=4), DCE-MRI overruled and was used as the gold standard.

Statistical Methods

Statistical analysis was performed by a statistician (__), using SPSS 24.0 (IBM Corp, Armonk, NY, USA). All calculations were performed on a per-lesion basis. Clustering effects due to several lesions were not taken into account. To account for skewed data, lesion size was described using median and range. To calculate sensitivity and specificity of DWI, DCE-MRI and mpMRI of the breast, the assigned final MR BI-RADS® classifications were dichotomized. BI-RADS® 1, 2, and 3 were considered benign. BI-RADS® 4 and 5 were considered malignant. Sensitivity, specificity, accuracy, negative predictive value (NPV), positive predictive value (PPV), area under the curve (AUC), and 95% confidence intervals (CI) for each parameter were calculated. Statistical differences between modalities and readers were assessed using General Estimation Equations. A p-value ≤0.05 was considered significant. Inter-reader variability for nominal and ordinal parameters was assessed by Fleiss' κ-statistics.

A sample size calculation using Nquery Advisor 7.0 (32) revealed that 102 cases are needed to obtain a power of 80% (alpha 5% two-sided) to detect the expected 7% difference in accuracy between DCE-MRI and DWI (given 8% discordant ratings).

Results

Histopathological diagnoses are summarized in Table 2. There were 69 malignant (median 20mm, range 6-100mm) and 41 benign tumors (median 16mm, range 8-100mm) in 106 patients (mean 51.6, 21-86 years). Four patients presented with bilateral lesions. Sensitivity, specificity, PPV, NPV, diagnostic accuracy, AUC for DCE-MRI, DWI and mpMRI for all readers and averages are summarized in Table 3. Detailed histopathological results and lesions sizes of false positives (FP) and false negatives (FN) with DCE-MRI, DWI, and mpMRI are detailed in Table 4.

DCE-MRI

DCE-MRI was the most sensitive technique for breast cancer detection with an average sensitivity of 100% with average NPV for breast cancer diagnosis of 99.9%. However, it had the greatest number of FPs with 12 (r1), 9 (r2), 11 (r3) and 7 (r4).

DWI

DWI detected significantly fewer breast cancers compared to both DCE-MRI ($p<0.0001$) as well as mpMRI ($p<0.0001$) with 11 (r1), 11 (r2), 15 (r3) and 13 (r4) FNs (Figures 1 and 2). Missed lesions with DWI were consistently ≤12mm in size (Figure 3) except for three invasive lobular carcinomas (ILC) (all readers: 25mm, r4: 26, 75mm) and two invasive ductal carcinomas (IDC) presenting as diffuse NME (r3,15mm, 18mm) and two mucinous carcinomas (all readers, 17mm, 38mm). Lesions ≤12mm in size comprised both invasive and non-invasive disease as well as all histopathological types (IDC, ILC, DCIS and mucinous) and tumor grades with the majority being rather intermediate and high grade. Average NPV of DWI (0.74) was significantly lower compared to DCE-MRI (0.99, $p<0.001$) and mpMRI (0.94, $p<0.001$).

DWI was significantly more specific than DCE-MRI ($p=0.002$) for lesion characterization with an average specificity of 86.8%. The PPV of DWI was significantly higher with an average of 91.2% compared to DCE-MRI and yet was not significantly different from mpMRI ($p=0.815$). DWI would have obviated 50% (6/12) for r1, 33.3% (3/9) for r2, 63.6% (7/11) for r3 and 85/7 % (6/7) for r4 of benign breast biopsies recommended with DCE-MRI alone. Therefore, DWI cannot be used as a stand-alone parameter for breast cancer detection in comparison to DCE-MRI or mpMRI.

mpMRI was significantly more sensitive than DWI and not significantly different from DCE-MRI ($p=0.120$). mpMRI ($p=0.009$) maintained the high specificity of DWI with an average of 83.8% ($p=0.195$) and was also more specific than DCE-MRI ($p=0.009$) (Figure 4). The PPV of mpMRI was significantly higher compared to DCE-MRI ($p=0.022$) and yet was not significantly different between DWI and mpMRI ($p=0.815$). mpMRI would have obviated 33.3% (4/12) for r1, 33.3% (3/9) for r2, 27.3% (3/11) for r3, 28.6% (2/7) for r4 of unnecessary breast biopsies recommended with DCE-MRI alone (Figure 5).

Diagnostic Accuracy

Receiving operator characteristic (ROC) curves for all readers and parameters are depicted in Figure 6. ROC analysis yielded the best AUC for mpMRI, compared to DCE-MRI, and DWI alone (Table 3).

The average diagnostic accuracy of mpMRI (91.9%) was higher than that of DCE-MRI (90.6%); although this didn't reach statistical significance ($p=0.466$), both mpMRI ($p=0.023$) and DCE-MRI ($p=0.002$) were significantly better than DWI with an average accuracy of 83.7%.

Intra- and inter-reader agreement

There was almost perfect inter-reader agreement for both DWI (benign vs. malignant) with κ =0.864 and for DCE-MRI (benign vs. malignant) with κ =0.875 and there was moderate inter-rater agreement for the assigned BI-RADS assessment category with κ =0.57.

There was no significant moderation of readers on parameters effects for either sensitivity (p=0.072), specificity (p=0.365), PPV (p=0.573), NPV (p=0.693) or diagnostic accuracy (p=0.750).

Discussion

DCE-MRI detects significantly more cancers than DWI (p<0.0001) with sensitivities decreasing especially in lesions ≤12mm or presenting as diffuse NME. Therefore, DWI cannot be used as a stand-alone parameter for breast cancer detection. mpMRI combining DWI and DCE-MRI achieves a high sensitivity and specificity, maximizing diagnostic accuracy and therefore obviating unnecessary breast biopsies in up to one-third of benign breast findings.

In this study DCE-MRI achieved the highest sensitivity for breast cancer detection for all readers ranging from 99-100%. This supports recent prior results that DCE-MRI is still superior to unenhanced MRI with or without supportive sequences (33). In addition, the results are in good agreement the existing body of evidence that DCE-MRI is the most sensitive test for breast cancer detection and outperforms conventional imaging methods in women, both with high and average risk of breast cancer (1, 34-36). Yet this excellent sensitivity comes at the expense of decreased specificity due to the also increased detection of benign lesions and a significant overlap of DCE-MRI features of benign and malignant lesions. This limitation causes unnecessary benign breast biopsies, patient anxiety and costs to the healthcare system.

Meanwhile DWI is emerging as a robust, sensitive and especially specific tool for unenhanced breast MRI (5, 6, 8). However, in most previous studies a high-resolution sequence to identify the breast lesion was a prerequisite for DWI interpretation, usually DCE-MRI (6, 8, 9, 22, 23, 30), and incidentally T2-weighted or T1-weighted unenhanced images (14, 17, 20). Thus, it was not assumed that the lesion could be identified directly on the DWI images. In our study, we found DWI detected significantly fewer cancers than DCE-MRI (p<0.0001), confirming that currently DWI cannot be used as a replacement for DCE-MRI in breast cancer detection.

Sensitivity is decreased in mass lesions ≦12mm regardless of invasiveness, histopathological type and grade and those presenting as diffuse NME regardless of size. It therefore appears the spatial resolution of DWI is still too low to be alone used for early detection. Current routine DCE-MRI easily achieves a spatial resolution of down to 1mm isotropic at 3T or even less at 7T (37), thereby reliably detecting these challenging lesions. On the other hand, the limited spatial resolution of DWI is therefore especially concerning in use for screening as the goal is early detection when lesions are still small and not yet metastasized (38). Research to improve spatial resolution of DWI is ongoing and there have been significant

improvements in spatial resolution with the introduction of read-out segmented EPI sequences (9). Therefore, it can be expected that further advances are possible and DWI in the future may be able to overcome its current limitations. In addition, other advanced DWI techniques such intravoxel incoherent motion, diffusion kurtosis imaging and diffusion tensor imaging are under investigation for their eventual role in breast imaging (39-42). Initial results indicate that there is potential to add further specificity to DCE, yet the clinical value of these additional techniques remains to be proven.

In our study mpMRI achieved the highest diagnostic accuracy for all readers from 91-93%. mpMRI obviates unnecessary breast biopsies in up to 33.3%, while the sensitivity for breast cancer is not significantly different from DCE-MRI, which is imperative. mpMRI is significantly more specific than DCE-MRI alone and this study, underscoring the necessity of combining DCE-MRI and DWI in a multiparametric imaging concept, which counter-balances the lack of sensitivity of DWI and the lack of specificity of DCE-MRI. Our results are in agreement with others who investigated mpMRI using different approaches to combine DWI and DCE-MRI and have demonstrated that mpMRI improves diagnostic accuracy (22-24).

Although DCE-MRI is the back-bone of any given imaging protocol, the recent controversy about the safety of gadolinium containing contrast agents (3) and the recommendation to use gadolinium contrast agents only when essential diagnostic information cannot be obtained with unenhanced scans, make the results of the current study particularly relevant (4). Our data indicate that for time being DWI with ADC mapping currently cannot be used as a stand-alone parameter for breast cancer detection yet, but as a complementary tool to DCE-MRI in a multiparametric MRI protocol to ensure breast cancer detection while decreasing unnecessary biopsies.

Although false-positives (FPs) were consistently reduced with mpMRI (27.3-33.3%), there remained some remained. These were comprised of up to four FP high-risk lesions, that per definition have an uncertain potential for malignancy (43). The decreased ADC values encountered in these FPs might reflect this potential or even an impending malignant transformation. Two FPs were clinically asymptomatic chronic abscesses, one fat necrosis and one fibrochystic changes, where ADCs might be decreased due to extensive fibrotic components. There were also some FN lesions with mpMRI. One FN was a mucinous carcinoma, that are known to present with very high ADC values due to their mucinous content (44). The other FNs comprised a small IDC and a ductal carcinoma in situ (DCIS) presenting as NME with borderline ADC values (45).

There was almost perfect inter-reader agreement for both DWI (benign vs. malignant) and DCE-MRI (benign vs. malignant). Readers were experienced breast radiologists with extensive training in breast MRI. Therefore, the results might not be applicable to every radiologist. However, our results are in good agreement with previous published data on high-resolution DCE-MRI and DWI (9, 30, 37). Our study is limited by the relatively small number of pure DCIS and ILC compared to the number of invasive ductal cancers, which limits specific insights into the performance of mpMRI in these subgroups. Nevertheless, the excellent results of mpMRI for both ILC and DCIS are in good agreement with previously

published data at 1.5T and 3T (25, 37) and therefore underline the potential of MpMRI when compared to DCE-MRI and DWI alone. It should be mentioned that as our institution is a referral center, this was an enriched cohort with all patients presenting with one (n=106) or two (n=4) lesions.

To date DWI cannot be used as a stand-alone parameter for breast cancer detection with sensitivities decreased in smaller cancers and those presenting as diffuse NME in comparison to DCE-MRI and mpMRI. DCE-MRI remains the most sensitive test for breast cancer detection and thus is still indispensable. mpMRI performed as the combination of DCE-MRI and DWI achieves both high sensitivity and specificity and should therefore be implemented into the standard MRI protocol to maximize diagnostic accuracy and while decreasing unnecessary breast biopsies.

Acknowledgments

Funding was provided by the Austrian Nationalbank ‘Jubiläumsfond’ Project Nr. 16219, the 2020 - Research and Innovation Framework Programme PHC-11-2015 Nr. 667211-2), and seed grants from Siemens Austria, Novomed, Medicor Austria, and Guerbet, France. This research was also funded in part through the NIH/NCI Cancer Center Support Grant P30 CA008748.

References

1. Mann RM, Balleyguier C, Baltzer PA, et al. Breast MRI: EUSOBI recommendations for women’s information. Eur Radiol. 2015
2. Kuhl CK. Current status of breast MR imaging. Part 2. Clinical applications. Radiology. 2007; 244(3):672–91. [PubMed: 17709824]
3. Runge VM. Safety of the Gadolinium-Based Contrast Agents for Magnetic Resonance Imaging, Focusing in Part on Their Accumulation in the Brain and Especially the Dentate Nucleus. Invest Radiol. 2016; 51(5):273–9. [PubMed: 26945278]
4. Runge VM. Critical Questions Regarding Gadolinium Deposition in the Brain and Body After Injections of the Gadolinium-Based Contrast Agents, Safety, and Clinical Recommendations in Consideration of the EMA’s Pharmacovigilance and Risk Assessment Committee Recommendation for Suspension of the Marketing Authorizations for 4 Linear Agents. Invest Radiol. 2017; 52(6): 317–23. [PubMed: 28368880]
5. Partridge SC, Nissan N, Rahbar H, et al. Diffusion-weighted breast MRI: Clinical applications and emerging techniques. J Magn Reson Imaging. 2017; 45(2):337–55. [PubMed: 27690173]
6. Dorrius MD, Dijkstra H, Oudkerk M, Sijens PE. Effect of b value and pre-admission of contrast on diagnostic accuracy of 1.5-T breast DWI: a systematic review and meta-analysis. Eur Radiol. 2014; 24(11):2835–47. [PubMed: 25103535]
7. Ouwerkerk R, Jacobs MA, Macura KJ, et al. Elevated tissue sodium concentration in malignant breast lesions detected with non-invasive 23Na MRI. Breast Cancer Res Treat. 2007; 106(2):151–60. [PubMed: 17260093]
8. Chen X, Li WL, Zhang YL, et al. Meta-analysis of quantitative diffusion-weighted MR imaging in the differential diagnosis of breast lesions. BMC Cancer. 2010; 10:693. [PubMed: 21189150]
9. Bogner W, Pinker-Domenig K, Bickel H, et al. Readout-segmented echo-planar imaging improves the diagnostic performance of diffusion-weighted MR breast examinations at 3.0 T. Radiology. 2012; 263(1):64–76. [PubMed: 22438442]
10. An YY, Kim SH, Kang BJ. Differentiation of malignant and benign breast lesions: Added value of the qualitative analysis of breast lesions on diffusion-weighted imaging (DWI) using readout-segmented echo-planar imaging at 3.0 T. PLoS One. 2017; 12(3):e0174681. [PubMed: 28358833]

11. Filli L, Ghafoor S, Kenkel D, et al. Simultaneous multi-slice readout-segmented echo planar imaging for accelerated diffusion-weighted imaging of the breast. Eur J Radiol. 2016; 85(1):274–8. [PubMed: 26547123]
12. Belli P, Bufi E, Bonatesta A, et al. Unenhanced breast magnetic resonance imaging: detection of breast cancer. Eur Rev Med Pharmacol Sci. 2016; 20(20):4220–9. [PubMed: 27831654]
13. Shin HJ, Chae EY, Choi WJ, et al. Diagnostic Performance of Fused Diffusion-Weighted Imaging Using Unenhanced or Postcontrast T1-Weighted MR Imaging in Patients With Breast Cancer. Medicine (Baltimore). 2016; 95(17):e3502. [PubMed: 27124054]
14. Trimboli RM, Verardi N, Cartia F, et al. Breast cancer detection using double reading of unenhanced MRI including T1-weighted, T2-weighted STIR, and diffusion-weighted imaging: a proof of concept study. AJR Am J Roentgenol. 2014; 203(3):674–81. [PubMed: 25148175]
15. McDonald ES, Hammersley JA, Chou SH, et al. Performance of DWI as a Rapid Unenhanced Technique for Detecting Mammographically Occult Breast Cancer in Elevated-Risk Women With Dense Breasts. AJR Am J Roentgenol. 2016; 207(1):205–16. [PubMed: 27077731]
16. Yabuuchi H, Matsuo Y, Sunami S, et al. Detection of non-palpable breast cancer in asymptomatic women by using unenhanced diffusion-weighted and T2-weighted MR imaging: comparison with mammography and dynamic contrast-enhanced MR imaging. Eur Radiol. 2011; 21(1):11–7. [PubMed: 20640898]
17. Baltzer PA, Benndorf M, Dietzel M, et al. Sensitivity and specificity of unenhanced MR mammography (DWI combined with T2-weighted TSE imaging, ueMRM) for the differentiation of mass lesions. Eur Radiol. 2010; 20(5):1101–10. [PubMed: 19936758]
18. Bickelhaupt S, Tesdorff J, Laun FB, et al. Independent value of image fusion in unenhanced breast MRI using diffusion-weighted and morphological T2-weighted images for lesion characterization in patients with recently detected BI-RADS 4/5 x-ray mammography findings. Eur Radiol. 2017; 27(2):562–9. [PubMed: 27193776]
19. Kul S, Oguz S, Eyuboglu I, Komurcuoglu O. Can unenhanced breast MRI be used to decrease negative biopsy rates? Diagn Interv Radiol. 2015; 21(4):287–92. [PubMed: 25835081]
20. Bickelhaupt S, Laun FB, Tesdorff J, et al. Fast and Noninvasive Characterization of Suspicious Lesions Detected at Breast Cancer X-Ray Screening: Capability of Diffusion-weighted MR Imaging with MIPs. Radiology. 2016; 278(3):689–97. [PubMed: 26418516]
21. Bickelhaupt S, Paech D, Laun FB, et al. Maximum intensity breast diffusion MRI for BI-RADS 4 lesions detected on X-ray mammography. Clin Radiol. 2017; 72(10):900 e1–e8.
22. Partridge SC, DeMartini WB, Kurland BF, et al. Quantitative diffusion-weighted imaging as an adjunct to conventional breast MRI for improved positive predictive value. AJR American journal of roentgenology. 2009; 193(6):1716–22. [PubMed: 19933670]
23. Ei Khouli RH, Jacobs MA, Mezban SD, et al. Diffusion-weighted imaging improves the diagnostic accuracy of conventional 3.0-T breast MR imaging. Radiology. 2010; 256(1):64–73. [PubMed: 20574085]
24. Baltzer A, Dietzel M, Kaiser CG, Baltzer PA. Combined reading of Contrast Enhanced and Diffusion Weighted Magnetic Resonance Imaging by using a simple sum score. Eur Radiol. 2016; 26(3):884–91. [PubMed: 26115653]
25. Pinker K, Bickel H, Helbich TH, et al. Combined contrast-enhanced magnetic resonance and diffusion-weighted imaging reading adapted to the “Breast Imaging Reporting and Data System” for multiparametric 3-T imaging of breast lesions. Eur Radiol. 2013; 23(7):1791–802. [PubMed: 23504036]
26. Pinker K, Bogner W, Baltzer P, et al. Improved differentiation of benign and malignant breast tumors with multiparametric 18fluorodeoxyglucose positron emission tomography magnetic resonance imaging: a feasibility study. Clin Cancer Res. 2014; 20(13):3540–9. [PubMed: 24963052]
27. Pinker K, Grabner G, Bogner W, et al. A combined high temporal and high spatial resolution 3 Tesla MR imaging protocol for the assessment of breast lesions: initial results. Invest Radiol. 2009; 44(9):553–8. [PubMed: 19652611]

28. Bickel H, Pinker K, Polanec S, et al. Diffusion-weighted imaging of breast lesions: Region-of-interest placement and different ADC parameters influence apparent diffusion coefficient values. Eur Radiol. 2017; 27(5):1883–92. [PubMed: 27578047]
29. Rosset A, Spadola L, Ratib O. OsiriX: An Open-Source Software for Navigating in Multidimensional DICOM Images. Journal of digital imaging. 2004; 17(3):205–16. [PubMed: 15534753]
30. Bogner W, Gruber S, Pinker K, et al. Diffusion-weighted MR for differentiation of breast lesions at 3.0 T: how does selection of diffusion protocols affect diagnosis? Radiology. 2009; 253(2):341–51. [PubMed: 19703869]
31. D'Orsi CJ, Sickles EA, Mendelson EB. , et al. ACR BI-RADS® Atlas, Breast Imaging Reporting and Data System. 5th. Reston, VA: American College of Radiology; 2013.
32. NQuery Advisor Version 7.0 [computer program]. 2007
33. Baltzer PAT, Bickel H, Spick C, et al. Potential of Noncontrast Magnetic Resonance Imaging With Diffusion-Weighted Imaging in Characterization of Breast Lesions: Intraindividual Comparison With Dynamic Contrast-Enhanced Magnetic Resonance Imaging. Invest Radiol. 2017
34. Riedl CC, Luft N, Bernhart C, et al. Triple-modality screening trial for familial breast cancer underlines the importance of magnetic resonance imaging and questions the role of mammography and ultrasound regardless of patient mutation status, age, and breast density. J Clin Oncol. 2015; 33(10):1128–35. [PubMed: 25713430]
35. Krammer J, Pinker-Domenig K, Robson ME, et al. Breast cancer detection and tumor characteristics in BRCA1 and BRCA2 mutation carriers. Breast Cancer Res Treat. 2017; 163(3): 565–71. [PubMed: 28343309]
36. Kuhl CK, Strobel K, Bieling H, et al. Supplemental Breast MR Imaging Screening of Women with Average Risk of Breast Cancer. Radiology. 2017; 283(2):361–70. [PubMed: 28221097]
37. Pinker K, Baltzer P, Bogner W, et al. Multiparametric MR Imaging with High-Resolution Dynamic Contrast-enhanced and Diffusion-weighted Imaging at 7 T Improves the Assessment of Breast Tumors: A Feasibility Study. Radiology. 2015:141905.
38. Saadatmand S, Bretveld R, Siesling S, Tilanus-Linthorst MM. Influence of tumour stage at breast cancer detection on survival in modern times: population based study in 173,797 patients. BMJ. 2015; 351:h4901. [PubMed: 26442924]
39. Cho GY, Moy L, Kim SG, et al. Evaluation of breast cancer using intravoxel incoherent motion (IVIM) histogram analysis: comparison with malignant status, histological subtype, and molecular prognostic factors. Eur Radiol. 2016; 26(8):2547–58. [PubMed: 26615557]
40. Sun K, Chen X, Chai W, et al. Breast Cancer: Diffusion Kurtosis MR Imaging-Diagnostic Accuracy and Correlation with Clinical-Pathologic Factors. Radiology. 2015; 277(1):46–55. [PubMed: 25938679]
41. Onaygil C, Kaya H, Ugurlu MU, Aribal E. Diagnostic performance of diffusion tensor imaging parameters in breast cancer and correlation with the prognostic factors. J Magn Reson Imaging. 2017; 45(3):660–72. [PubMed: 27661775]
42. Bokacheva L, Kaplan JB, Giri DD, et al. Intravoxel incoherent motion diffusion-weighted MRI at 3.0 T differentiates malignant breast lesions from benign lesions and breast parenchyma. J Magn Reson Imaging. 2014; 40(4):813–23. [PubMed: 24273096]
43. Riedl CC, Ponhold L, Flory D, et al. Magnetic resonance imaging of the breast improves detection of invasive cancer, preinvasive cancer, and premalignant lesions during surveillance of women at high risk for breast cancer. Clin Cancer Res. 2007; 13(20):6144–52. [PubMed: 17947480]
44. Woodhams R, Kakita S, Hata H, et al. Diffusion-weighted imaging of mucinous carcinoma of the breast: evaluation of apparent diffusion coefficient and signal intensity in correlation with histologic findings. AJR American journal of roentgenology. 2009; 193(1):260–6. [PubMed: 19542422]
45. Iima M, Le Bihan D, Okumura R, et al. Apparent diffusion coefficient as an MR imaging biomarker of low-risk ductal carcinoma in situ: a pilot study. Radiology. 2011; 260(2):364–72. [PubMed: 21633054]

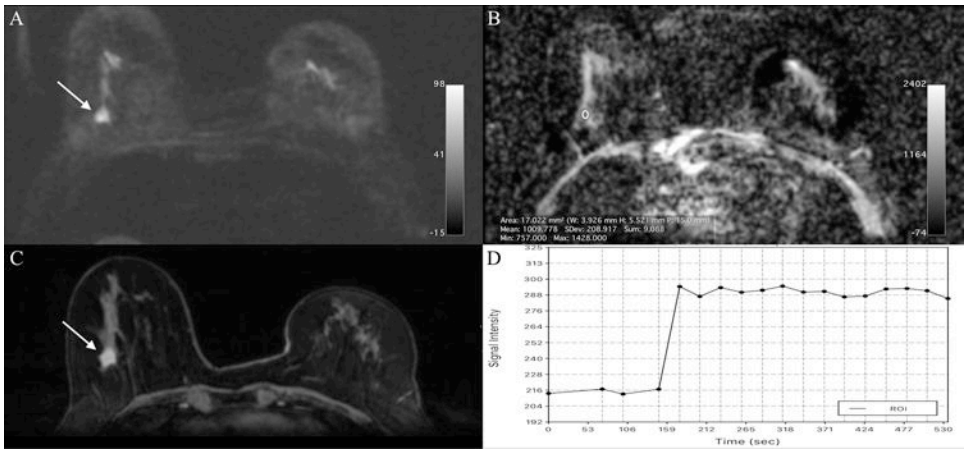

Figure 1.

Invasive ductal carcinoma (IDC) grade 1 laterally in the right breast in a 63-year-old woman: (A) On DWI in the high b-value images there are restricted diffusivity (arrow) and (B) decreased ADC values (1.009×10^{-3} mm^2/s) evident; thus DWI findings were classified as positive for malignancy. On DCE-MRI there is a 13mm (C) irregular shaped and partly spiculated mass with (D) an initial fast heterogeneous contrast enhancement followed by a plateau; thus DCE-MRI findings were classified as BI-RADS 5. DWI accurately detected this breast cancer.

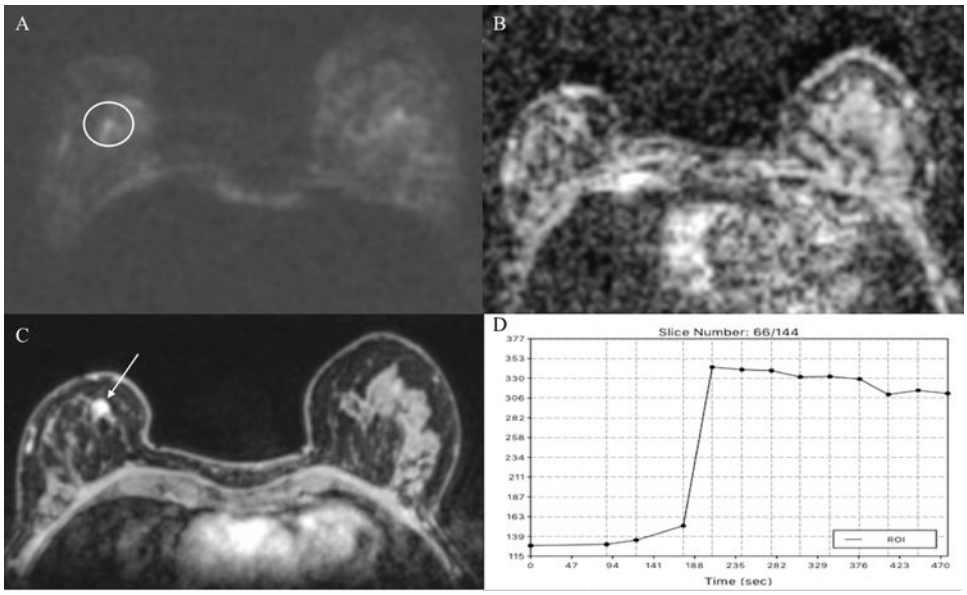

Figure 2.

Invasive ductal carcinoma (IDC) grade 3 medially retro-areolar in the right breast in a 64-year-old woman: (A) On DWI in the high b-value images there is no restricted diffusivity or (B) decreased ADC values evident; DWI findings were classified as negative for malignancy. However, on DCE-MRI there is a (C) round and partly irregularly marginated mass 12 o'clock in the right breast (arrow) with (D) an initial fast slightly heterogeneous contrast enhancement followed by a plateau and was classified as BI-RADS 4. DWI was false negative.

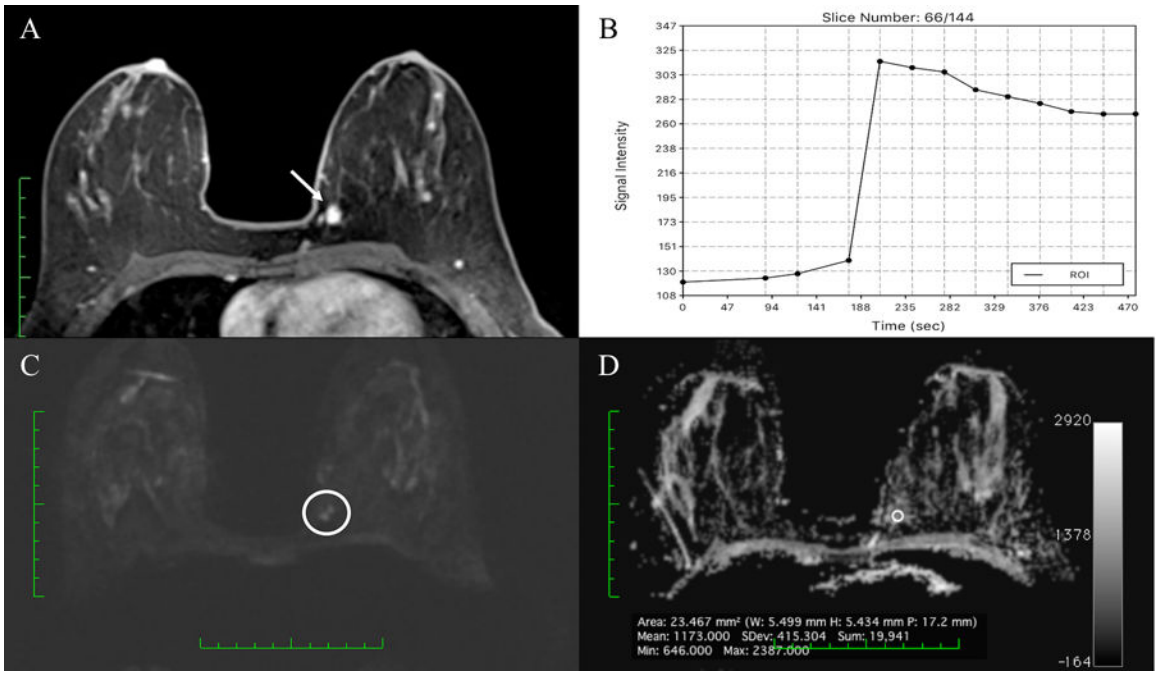

Figure 3.

Invasive ductal carcinoma (IDC) G3 in the left breast medial in a 45-year-old woman. (A) On DCE-MRI there is an 8mm irregular-shaped and partially irregularly marginated lesion (arrow) with (B) an initial fast/wash-out enhancement (III); DCE-MRI findings were classified as highly suggestive for malignancy (BI-RADS 5). DWI was false negative as none of the readers called this lesion on DWI alone. However when read as mpMRI combining DCE-MRI and DWI, readers identified a (C) hyperintense correlate (circle) with (D) ADC values measuring 1.173×10^{-3} mm2/s, which further confirmed malignancy.

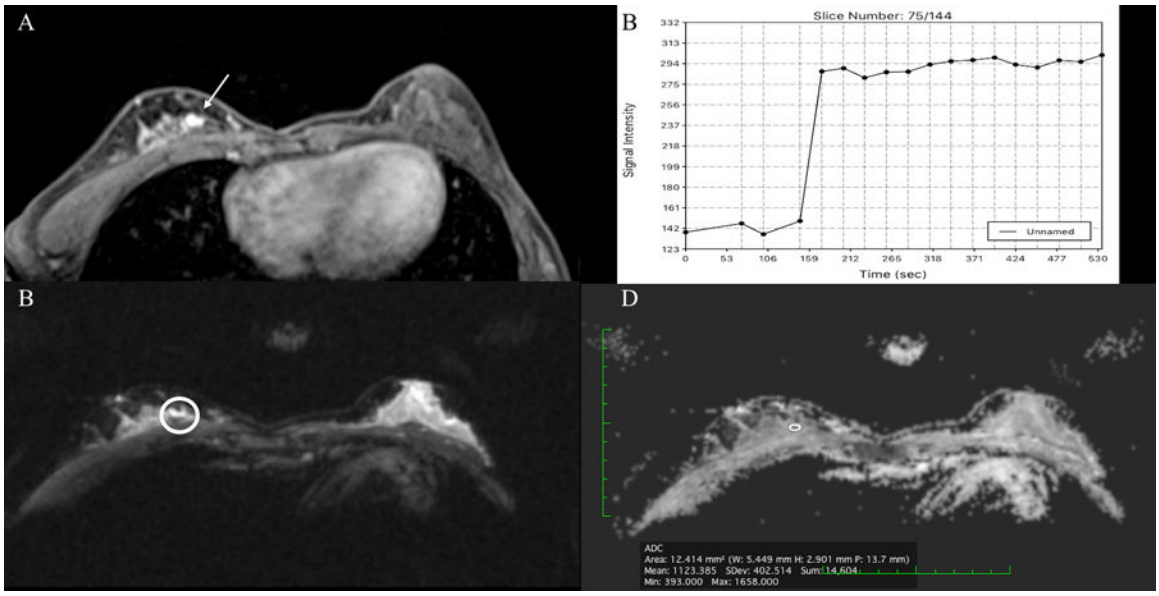

Figure 4.

Invasive ductal carcinoma in a 41-year-old woman grade 3, medially in the right breast (arrow). In the initial independent review of DWI all readers scored negative for malignancy. (A) On DCE-MRI there is a 8mm circumscribed, oval lesion demonstrating (B) an initial fast/persistent (II) heterogeneous contrast enhancement, that was classified as probably benign (BI-RADS 3). However, when interpreted as mpMRI, reader acknowledged a (C) restricted diffusivity (circle) and (D) decreased ADC values (1.1123×10^{-3} mm^2/s) for the enhancing mass. mpMRI using the combined information of both DCE-MRI accurately classified this lesion as malignant.

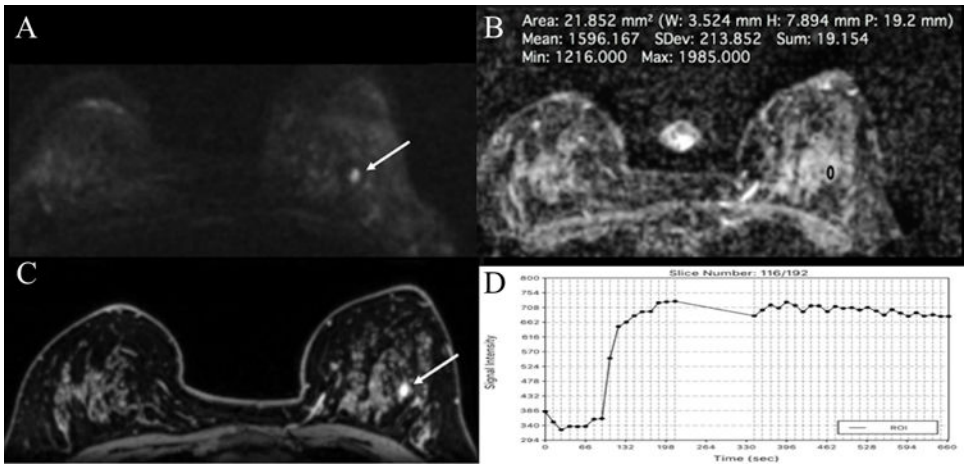

Figure 5.

Fibroadenoma in a 42-year-old woman, centro-lateral in the left breast: (A-C) The irregular-shaped and partially irregularly marginated 7mm mass demonstrates (D) an initial fast/plateau (II) slightly heterogeneous contrast enhancement. (E) On DWI, the mass is bright on b=850 images due to "T2-shine through, but has (F) no decreased ADC values (1.596×10^{-3} mm^2/s). DCE-MRI and DWI were discordant. According to the BI-RADS-adapted reading algorithm, the BI-RADS assessment category assigned based on DCE-MRI was overruled and multiparametric MRI correctly classified the mass as benign.

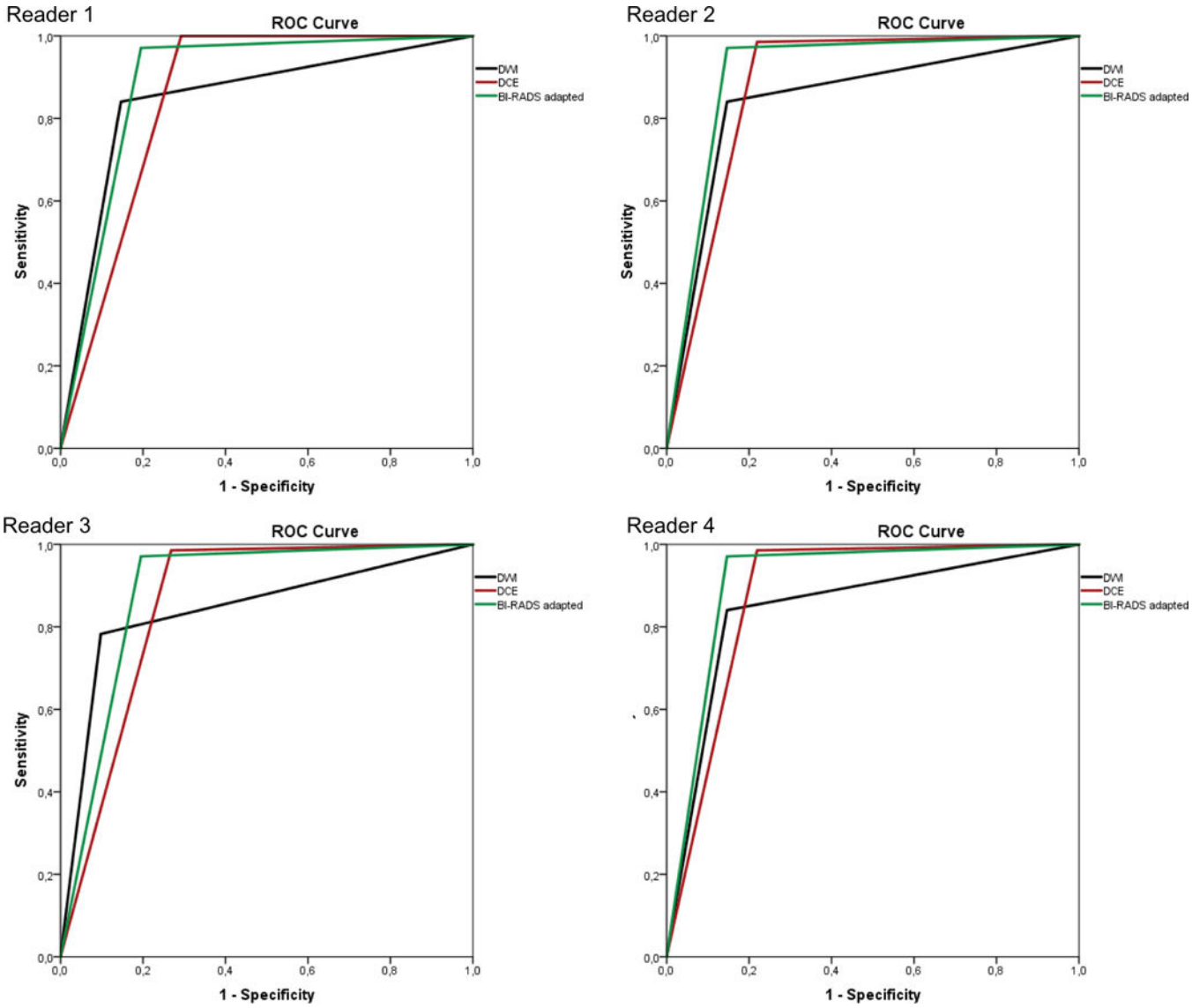

Figure 6.

Receiver operating characteristic (ROC) analysis for all readers and parameters.

ROC curves illustrate the higher diagnostic value (i.e. higher sensitivity, specificity and larger area under the curve) that was reached for mpMRI using the BI-RADS®-adapted reading method, compared with DCE-MRI and DWI alone for all readers.

Table 1

ADC thresholds for mpMRI with DCE-MRI and DWI, using the BI-RADS-adapted reading algorithm.

BI-RADS assessment categories	ADC threshold ($\times 10^{-3}$ mm^2/s) for upgrade to positive for malignancy	
	mass	NME
BI-RADS 1	≤0.61	≤0.28
BI-RADS 2	≤0.87	≤0.62
BI-RADS 3	≤1.13	≤0.95
BI-RADS 4	≤1.39	≤1.28
BI-RADS 5	≤1.66	≤1.62

Modified from Ref12.

Note- ADC=Apparent diffusion coefficient, BI-RADS = Breast Imaging Reporting and Data System, DCE= Dynamic contrast-enhanced, MRI= Magnetic resonance imaging, mp=Multiparametric, DWI= Diffusion-weighted imaging, NME=Non-mass enhancement

Table 2

Histopathological diagnoses for benign and malignant breast lesions

Histopathological subtype	**n**	**%**
Malignant	69	62.7
IDC	59	53.6
ILC	3	2.7
Ductal carcinoma in situ (DCIS)	4	3.6
Mucinous	2	1.9
Myelosarcoma	1	0.9
Benign	41	37.3
High risk (ADH, sclerosing adenosis with atypia, metaplasia with atypia, complex sclerosing lesion, CCC with focal atypia)	7	6.4
FA/FAH	22	20
Apocrine metaplasia	2	1.9
DH, CCC, FCC, focal fibrosis, nodular sclerosing adenosis	5	4.5
Miscellaneous (fat necrosis, cyst with inflammation)	5	4.5

Note- ADH= Atypical ductal hyperplasia, DCIS= Ductal carcinoma in situ, IDC= Invasive ductal carcinoma, DH= Ductal hyperplasia, CCC= Columnar cell changes, FA= Fibroadenoma, FAH= Fibroadenomatous hyperplasia, FCC= Fibrochystic changes, ILC= Invasive lobular carcinoma

Table 3

Sensitivity, specificity, PPV, NPV, diagnostic accuracy, AUC for DCE-MRI, DWI and mpMRI for all readers

	MRI parameters	Sensitivity	CI	Specificity	CI	PPV	CI	NPV	CI	Accuracy	CI	AUC
r1	DCE-MRI	1	1	0.71	0.55–0.83	0.85	0.76–0.92	1	1	0.89	0.82–0.94	0.85
	DWI	0.84	0.74–0.91	0.85	0.71–0.93	0.91	0.81–0.96	0.76	0.62–0.86	0.85	0.77–0.91	0.85
	MpMRI	0.97	0.89–0.99	0.81	0.66–0.9	0.89	0.8–0.95	0.94	0.8–0.96	0.91	0.84–0.95	0.89
r2	DCE-MRI	0.99	0.9–0.99	0.78	0.63–0.88	0.88	0.79– 0.94	0.97	0.81–0.99	0.91	0.84–0.95	0.88
	DWI	0.84	0.73–0.91	0.85	0.71–0.93	0.91	0.81–0.96	0.76	0.62–0.86	0.85	0.77–0.91	0.85
	MpMRI	0.97	0.9–0.99	0.85	0.71–0.93	0.92	0.83–0.96	0.95	0.81–0.99	0.93	0.86–0.96	0.91
r3	DCE-MRI	0.99	0.9–0.99	0.73	0.58 0.85	0.86	0.80–0.95	0.97	0.8–0.99	0.89	0.82–0.94	0.86
	DWI	0.78	0.67–0.86	0.9	0.77–0.96	0.93	0.83–0.97	0.71	0.58–0.82	0.83	0.75–0.89	0.84
	MpMRI	0.97	0.89–0.99	0.81	0.66–0.89	0.89	0.97–0.94	0.94	0.8–0.99	0.91	0.84–0.95	0.89
r4	DCE-MRI	0.99	0.9–0.99	0.83	0.68–0.92	0.89	0.80–0.96	0.97	0.82–0.99	0.93	0.86–0.96	0.91
	DWI	0.81	0.7–0.89	0.85	0.74–0.95	0.9	0.82–0.95	0.73	0.59–0.84	0.83	0.75–0.89	0.83
	MpMRI	0.96	0.87–0.99	0.88	0.74–0.95	0.93	0.84–0.97	0.92	0.79–0.98	0.93	0.86–0.96	0.92
Average	DCE-MRI	1	0.99–1	0.77	0.63–0.86	0.91	0.80–0.93	0.99	0.99–1	0.91	0.84–0.94	na
	DWI	0.81	0.7–0.89	0.87	0.75–0.93	0.9	0.82–0.96	0.74	0.61–0.84	0.83	0.76–0.89	na
	MpMRI	0.97	0.89–0.99	0.84	0.7–0.94	0.93	0.82–0.96	0.94	0.8–0.98	0.92	0.86–0.96	na

Note- AUC= Area under the curve, CI= 95% Confidence interval, DWI= Diffusion-weighted imaging, DCE= Dynamic contrast-enhanced, MRI= Magnetic resonance imaging, na= not applicable, mp= multiparametric, NPV= Negative predictive value, PPV= Positive predictive value, R= Reader

Table 4

Histopathological results and lesions sizes of false positives (FP) and false negatives (FN) with DCE-MRI, DWI, and mpMRI

	MRI parameters	False positives	size median (range) mm	n	False negatives	size median (range) mm	n
r1	**DCE-MRI**	2 Chronic abscess	82.5 (80–85)	**12**			**0**
		3 FA	13 (11–39)				
		1 Fat necrosis	15				
		1 FCC	19				
		4 High risk	28.5 (22–37)				
		1 Metaplasia	12				
	DWI	2 Chronic abscess	82.5 (80–85)	**6**	7 IDC	8 (6–12)	**11**
		1 Fat necrosis	15		1 ILC	25	
		3 High risk	27 (22–30)		2 Mucinous	27.5 (17–38)	
					1 DCIS	7	
	mpMRI	2 Chronic abscess	82.5 (80–85)	**8**	1 IDC	9	**2**
		1 Fat necrosis	15		1 Mucinous	38	
		1 FCC	19				
		4 high risk	28.5 (22–37)				
r2	**DCE-MRI**	2 Chronic abscess	82.5 (80–85)	**9**	1 IDC	10	**1**
		1 FA	39				
		2 Fat necrosis	13.5 (12–15)				
		3 High risk	26 (22–27)				
		1 Metaplasia	12				
	DWI	2 Chronic abscess	82.5 (80–85)	**6**	8 IDC	8.5 (6–15)	**11**
		1 Fat necrosis	15		1 ILC	25	
		1 cyst with inflammation	10		2 Mucinous	27.5 (17–38)	
		2 High risk	24.5 (22–27)				
	mpMRI	2 Chronic abscess	82.5 (80–85)	**6**	1 IDC	9	**2**
		1 Fat necrosis	15		1 Mucinous	38	
		3 High risk	27 (22–30)				

	MRI parameters	False positives	size median (range) mm	n	False negatives	size median (range) mm	n
r3	**DCE-MRI**	2 Chronic abscess	82.5 (80–85)	**11**	1 IDC	10	**1**
		2 FA	29 (13–39)				
		1 Fat necrosis	15				
		1 FCC	19				
		4 High risk	26.5 (22–37)				
		1 Metaplasia	12				
	DWI	1 Chronic abscess	80	**4**	11 IDC	9 (6–18)	**15**
		1 Fat necrosis	15		1 ILC	25	
		2 High risk	24.5 (22–27)		2 Mucinous	27.5 (17–38)	
					1 DCIS	7	
	mpMRI	2 Chronic abscess	82.5 (80–85)	**8**	1 IDC	9	**2**
		1 Fat necrosis	15		1 Mucinous	38	
		1 FCC	19				
		4 High risk	26.5 (22–37)				
r4	**DCE-MRI**	2 Chronic abscess	82.5 (80–85)	**7**	1 DCIS	7	**1**
		1 FAH	19				
		1 Fat necrosis	15				
		3 High risk	27 (22–30)				
	DWI	2 Chronic abscess	82.5 (80–85)	**6**	7 IDC	9 (8–12)	**13**
		1 FAH	19		3 ILC	26 (25–75)	
		3 High risk	27 (22–30)		2 Mucinous	27.5 (17–38)	
					1 DCIS	7	
	mpMRI	2 Chronic abscess	82.5 (80–85)	**5**	1 IDC	9	**3**
		3 High risk	27 (22–30)		1 Mucinous	38	
					1 DCIS	7	

Note- DWI= Diffusion-weighted imaging, DCE= Dynamic contrast-enhanced, DCIS= Ductal carcinoma in situ, IDC= Invasive ductal carcinoma, FA= Fibroadenoma, FAH= Fibroadenomatous hyperplasia, FCC= Fibrochystic changes, ILC= Invasive lobular carcinoma, MRI= Magnetic resonance imaging, mp= Multiparametric, R= Reader